Creation of NV centers over a millimeter-sized region by intense single-shot ultrashort laser irradiation ⒡

(iD) Masanori Fujiwara, (iD) Shunsuke Inoue, Shin-ichiro Masuno, et al.

COLLECTIONS

Note: This paper is part of the APL Photonics Special Topic on Ultrafast Laser Fabrication Enabled Photonics and Devices.

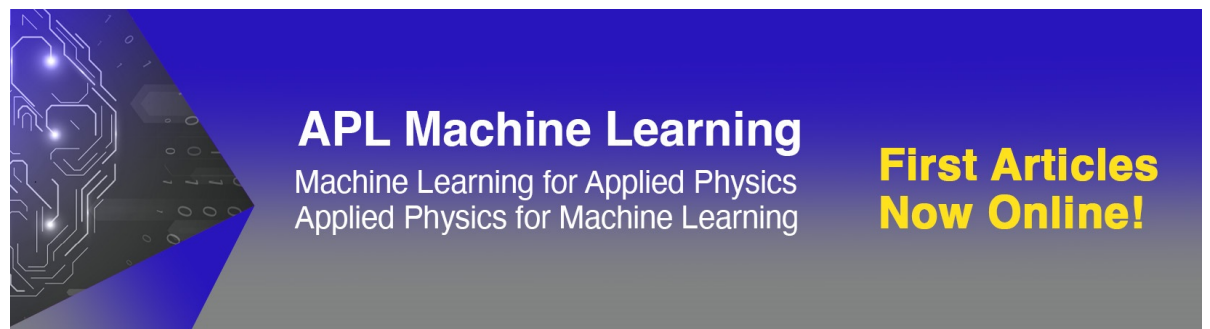⒡ This paper was selected as Featured

open access

View Online   Export Citation   CrossMark

APL Machine Learning
Machine Learning for Applied Physics
Applied Physics for Machine Learning

First Articles Now Online!

AIP Publishing

Creation of NV centers over a millimeter-sized region by intense single-shot ultrashort laser irradiation Ⓕ

View Online   Export Citation   CrossMark

Masanori Fujiwara,[1] ⒾⒹ Shunsuke Inoue,[1] ⒾⒹ Shin-ichiro Masuno,[1] Haining Fu,[1] Shigeki Tokita,[1] ⒾⒹ
Masaki Hashida,[1,2] ⒾⒹ and Norikazu Mizuochi[1,3,4,a)] ⒾⒹ

AFFILIATIONS

[1] Institute for Chemical Research, Kyoto University, Gokasho, Uji, Kyoto 611-0011, Japan
[2] Research Institute of Science and Technology, Tokai University, 4-1-1 Kitakaname, Hiratsuka, Kanagawa 259-1292, Japan
[3] Center for Spintronics Research Network, Kyoto University, Gokasho, Uji, Kyoto 611-0011, Japan
[4] International Center for Quantum-field Measurement Systems for Studies of the Universe and Particles (QUP), KEK, Tsukuba, Ibaraki 305-0801, Japan

Note: This paper is part of the APL Photonics Special Topic on Ultrafast Laser Fabrication Enabled Photonics and Devices.
[a)]Author to whom correspondence should be addressed: mizuochi@scl.kyoto-u.ac.jp. **Tel.:** +81-774-38-3130

ABSTRACT

Recently, ultrashort laser processing has attracted attention for creating nitrogen-vacancy (NV) centers because this method can create single NV centers in spatially-controlled positions, which is an advantage for quantum information devices. On the other hand, creating high-density NV centers in a wide region is also important for quantum sensing because the sensitivity is directly enhanced by increasing the number of NV centers. A recent study demonstrated the creation of high-density NV centers by irradiating femtosecond laser pulses, but the created region was limited to micrometer size, and this technique required many laser pulses to avoid graphitization of diamond. Here, we demonstrate the creation of NV centers in a wide region using only an intense single femtosecond laser pulse irradiation. We irradiated a diamond sample with a femtosecond laser with a focal spot size of 41 μm and a laser fluence of up to 54 J/cm^2, which is much higher than the typical graphitization threshold in multi-pulse processing. We found that single-pulse irradiation created NV centers without post-annealing for a laser fluence higher than 1.8 J/cm^2, and the region containing NV centers expanded with increasing laser fluence. The diameter of the area was larger than the focal spot size and reached over 100 μm at a fluence of 54 J/cm^2. Furthermore, we demonstrated the NV centers' creation in a millimeter-sized region by a single-shot defocused laser pulse over 1100 μm with a fluence of 33 J/cm^2. The demonstrated technique will bring interest in the fundamentals and applications of fabricating ultrahigh-sensitivity quantum sensors.

I. INTRODUCTION

Nitrogen-vacancy (NV) centers in diamond have attracted interest in the field of quantum science and technology.[1–5] NV centers have long spin coherence times even at room temperature,[6] and their spin state can be optically read out and manipulated. In quantum sensing with NV centers, magnetic[7–9] and electric fields,[10] temperature,[11,12] pressure,[13] and pH[14] can be sensed with a high dynamic range.[15]

Recently, the formation of single NV centers by femtosecond laser irradiation has been reported.[16–18] In the reported study,

femtosecond laser irradiation first created vacancies, which were moved by thermal treatment or by repeated laser pulse irradiation. The NV centers were created by the recombination of vacancies and substitutional nitrogen in the vicinity of the focal point. In addition, the detailed generation mechanism of vacancy–interstitials pairs was investigated using a theoretical approach.[19] Compared with other methods such as electron or ion implantation, femtosecond laser direct writing has the benefit of being able to realize a flexible spatial arrangement of NV centers in three dimensions by controlling the shape of the focal spot.[16–18,20,21] Furthermore, compared with high-energy electron irradiation, it does not emit dangerous radiation

such as x rays. By utilizing these advantages, the laser writing technique is now widely applied to create different color centers in other optical materials,[22] such as hexagonal boron nitride,[23] gallium nitride,[24] and silicon carbide.[25]

For quantum sensing, creating high-density NV centers in a wide region is also important for enhancing sensitivity. This is because the sensitivity scales with $\sqrt{N}$, where N is the number of NV centers used for the sensing measurement.[7] High-density NV centers are also an excellent model for exploring quantum many-body physics.[26–28] For example, the magnetic sensitivity using ensemble NV centers is currently realized to 0.9 pT/$\sqrt{\text{Hz}}$ (AC field)[29] and 15 pT/$\sqrt{\text{Hz}}$ (DC field)[30] even at room temperature. The attainable sensitivity of the high-density NV ensemble is expected to be at the femto-to atto-tesla level at room temperature, comparable to that of ultra-sensitive sensors such as superconducting quantum interference devices.[31] In addition, large-size diamond sensors are now powerful tools for widefield quantum sensing.[27,32] As an excellent biological application, millimeter-scale magnetocardiography (detection of the magnetic field induced by the cardiac current in the heart) in living rats was realized using a five-millimeter-sized NV diamond.[33]

A recent study demonstrated the creation of high-density NV centers in a micrometer-sized region by illuminating it with many laser pulses.[34] However, this method requires a long irradiation time for NV creation in a wide region. Creating NV centers in a wide region using a few laser pulses is attractive in scientific studies and industrial applications, but is a challenging problem. To avoid diamond graphitization, conventional methods focus many laser pulses with low laser fluence on a narrow region using high-numerical-aperture (NA) optics.[17,34,35] To verify whether NV centers can be created by only a few pulses in a wide region, high-fluence laser pulses should be focused using low-NA optics. This condition will require a femtosecond laser with high pulse energy and a properly-controlled pulse number.

In the current Letter, we investigate the creation of NV centers in diamond by highly intense femtosecond laser irradiation with a Ti:sapphire chirped-pulse amplification (CPA) laser system.[36] Our CPA system can control the pulse number and realize high fluence even with a large focal spot size. We focused the laser pulses on a diamond surface with various conditions (focal shape, laser fluence, and pulse number). After the surface cleaning with boiling acid, we found that single-pulse irradiation creates NV centers without post-annealing when the laser pulse is larger than the typical graphitization threshold. We found the region containing NV centers expanded by increasing the laser fluence. Finally, we will report that NV centers were created in a millimeter-sized area using a defocused spot with high pulse energy.

II. EXPERIMENTAL

A. Sample information

Three diamond substrates, No. 1, No. 2, and No. 3, were used for laser irradiation experiments. All the substrates have the same material properties, that is, a high-pressure–high-temperature (HPHT) Ib (001) diamond ([N] ~ 100 ppm) with a natural abundance of ^{13}C isotope (1.1%). The diamond sizes were $4 \times 4 \times 0.3$ mm^3

for No. 1, $3 \times 1.5 \times 0.3$ mm^3 for No. 2, and $2 \times 2 \times 0.3$ mm^3 for No. 3.

B. Femtosecond laser irradiation system

Figure 1(a) shows a schematic of the fs-laser irradiation system. The femtosecond laser irradiation was performed using a Ti:Sapphire CPA system (pulse width = 35 fs, center wavelength λ = 810 nm, repetition rate = 10 Hz, maximum pulse energy = 500 mJ).[36] The pulse energy was changed by an attenuator consisting of a half-wave plate and a polarizing beam splitter in the laser system. The beam size and shape were adjusted by an iris diaphragm or an optical slit. While the energy was changed by rotating the wave plate, the size and shape were maintained. After the adjustment, the laser beam was focused onto a diamond substrate by an off-axis parabolic mirror with a focal length of 165 mm. The laser polarization was set to a linear polarization almost parallel to [100] or [010]. In this case, the angles between the polarization orientation and all the possible NV axial orientations (NV || [111] or [$1\bar{1}\bar{1}$] or [$\bar{1}1\bar{1}$] or [$\bar{1}\bar{1}1$]) became the same. We prepared two focal spots at the sample position, that is, circle-shaped spots and line-shaped spots, as shown in Figs. 1(b) and 1(c). These spot images were monitored using a complementary-metal-oxide-semiconductor (CMOS) camera with a lens pair system in advance. Each spot diameter ($2w_x$, $2w_y$) ($1/e^2$ full width in the horizontal and vertical directions) was (41, 41 μm) and (151, 4.2 μm) from a 2D Gaussian curve fit. Before the laser irradiation, the laser energy (the laser fluence) was confirmed by a pyroelectric energy sensor placed between the parabolic mirror and the sample. As mentioned below, our laser fluence is much higher than the graphitization threshold. The high fluence irradiation will induce several defects, such as graphite or amorphous carbon, on the diamond surface. Therefore, the sample substrates were cleaned by mixed boiling acid (HNO$_3$:H$_2$SO$_4$ = 1:3, 200 °C for 1.5 h) to remove these defects after the laser irradiation.

C. Confocal optical system

The laser-irradiated regions were observed using a custom-built confocal microscope. A continuous-wave (CW) green laser
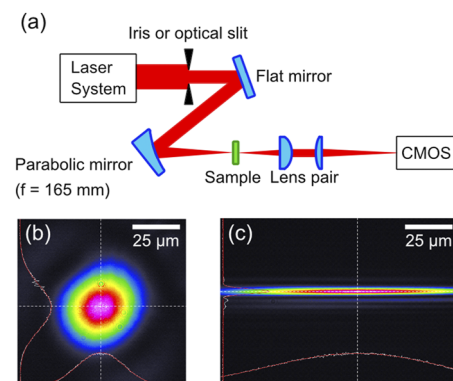

FIG. 1. (a) Schematic setup for irradiation with ultrashort laser pulses on a diamond substrate. (b) and (c) Images of a circular and linear laser spot at the focal position confirmed by the CMOS camera.

beam (λ = 532 nm) was focused onto the diamond by an oil-immersion objective lens (NA = 1.45). The excitation laser power was set to 100 μW, measured before the objective. The photoluminescence (PL) from the sample was collected by the same objective, filtered by a 552-nm dichroic mirror, and passed through a 50 μm pinhole. The signal was introduced to either a single-photon counting module for a PL image or a Czerny–Turner monochromator for a PL spectrum. The position of the objective lens was controlled by a three-axis piezo stage (25 μm for the optical axial direction and 100 × 100 μm^2 for the horizontal region). After 2D raster scanning at the optimal axial position, we obtained a confocal image of the laser-irradiated region. The lateral and axial resolutions D_R and Z_R of the confocal system were 400 and 1500 nm, respectively, evaluated by the full width at half maximum (FWHM) of the intensity distribution for each direction. We calculated the effective focal volume V_E as $V_E = \pi \times (D_R/2)^2 \times Z_R = 2 \times 10^{-13}$ cm^3, according to the analysis given by Ref. 34. For the PL spectrum measurement at the target position, we used a 150 gr/mm diffraction grating placed in the monochromator. The spectral range was 350 nm and the resolution was 0.6 nm.

III. RESULTS AND DISCUSSIONS

A. Creation of NV centers by a single laser pulse

We first examined the pulse number dependence of NV center creation. Figure 2(a) shows an optical micrograph of the diamond surface after fs-laser irradiation. In this experiment, diamond substrate No. 1 was used. The upper and lower sides show a series of circular- and linear-spot-irradiated regions for different input pulse numbers N. The laser fluence F was fixed at 5 J/cm^2 for the circular spots and 26 J/cm^2 for the linear spots. Due to laser-induced graphitization, the irradiated regions were more ablated and became darker with increasing N. Figures 2(b)–2(d) show confocal scans for circular spots for N = 1, 5, and 10 after the acid cleaning process. Each image has a bright circular region with a width of more than 25 μm. The region for N = 1 shows a higher PL intensity than the regions for N = 5 and 10. Figures 2(e)–2(g) show typical PL spectra obtained from the centers of the bright regions in Figs. 2(b)–2(d). The spectrum for N = 1 clearly shows spectral features associated with NV centers.[5,37–42] Compared with the spectrum for N = 1, the spectra for N = 5 and 10 have lower PL intensity, which indicates that the creation efficiency of the NV centers becomes low due to the increase of the laser ablation. Note the peaks at around 575 and 630 nm in the spectra that emerged regardless of the pulse number, and they are the Raman peaks from the diamond crystal.[37]

Figures 2(h)–2(m) show images of linear-spot-irradiated regions for N = 1, 5, and 10, and PL spectra obtained near the centers of these irradiated regions. The results for the linear spots showed the same trend as those for the circular spots. Line-shaped regions that reflect the line spots were observed on the diamond surface. The region for N = 1 showed a high concentration of NV centers. From a Gaussian fit, the size of the irradiated region for N = 1 was estimated to be 51 × 4 μm^2. This shows that for a focal spot line-scanned on a diamond surface, NV centers can be rapidly generated in a wide region without post-annealing.

Creating NV centers with only a single laser pulse has not yet been reported. According to previous studies, the first pulse creates lattice vacancies (GR1 centers), and subsequent processes, such as
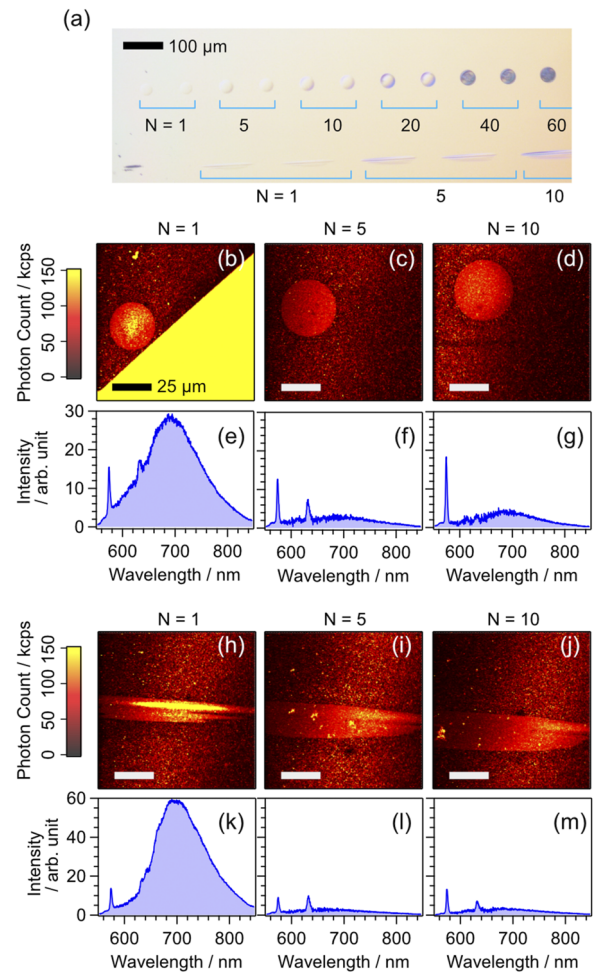

FIG. 2. (a) Series of fs-laser irradiated regions with various pulse numbers N. The upper side is a series of circular laser spots with a fluence of F = 5 J/cm^2 and the lower side is for linear laser spots with F = 26 J/cm^2. (b)–(d) Confocal images at the circular-spot-irradiated regions for N = 1, 5, and 10. Note that the triangular region with high PL intensity in Fig. (b) corresponds to a bright structure in the sample and is unrelated to the fs-laser irradiation. (e)–(g) PL spectra around the centers of the irradiated regions of (b)–(d). (h)–(j) and (k)–(m) are confocal images and their PL spectra for the linear spots.

thermal annealing[16,18] or illumination with a laser pulse train,[17,34,35] create more vacancies or combine existing vacancies with substitutional nitrogen atoms. In the current work, however, the NV centers were created by single-pulse irradiation. This differs from previous experiments in that (1) the laser fluence was higher than the typical threshold for diamond graphitization (1–4 J/cm^2, depending on several factors such as the pulse width, pulse number, and center wavelength),[43–47] and (2) the laser pulse was loosely focused (NA ~ 0.02) to obtain a large focal spot. Irradiating a single pulse onto a pristine diamond surface, both vacancy creation and N-V combination may occur together at a depth near the laser-ablated region. In contrast, multi-pulse irradiation will promote diamond graphitization and prevent the effective creation of NV centers due to the change in optical properties at the surface.[44,48]

The concentration of NV centers at the highest PL intensity positions in the circular and linear spot irradiated regions for $N = 1$ [Figs. 2(b) and 2(h)] was estimated to be 1.5×10^{13} and 3.5×10^{13} cm^{-3}, respectively. The typical concentration in a laser-irradiated region is $\sim 1 \times 10^{13}$ cm^{-3}. This concentration was calculated by comparison with the previously reported PL intensity for a single NV center in the effective focal volume V_E.[34] Note, first, that this estimation depends on the detection efficiency and spatial resolution of the microscope. Second, generated NV centers were found only at the diamond surface within the axial resolution Z_R of the system. Since the actual focal volume must be smaller than the effective focal volume, the actual NV center concentration will be higher than our estimation. Third, comparing the two images, the line-spot-irradiated region has a higher NV concentration than the circle-spot-irradiated region. The differences in the laser fluence as well as the shape of the focusing beam may influence NV center generation.

B. Laser fluence dependence

We next investigated the dependence on the fs-laser fluence. Figure 3(a) shows a series of circular-spot-irradiated regions for various fluences F ranging from 1.1 to 54 J/cm^2 on diamond substrate No. 2. The pulse number N was fixed at 1 for each region. Figures 3(b)–3(l) show confocal images of the laser-irradiated regions, indicated by dotted circles in Fig. 3(a). In Fig. 3(b), for $F = 1.1$ J/cm^2, there was no region with an increased PL intensity. However, higher-intensity regions for $F > 1.8$ J/cm^2 are present in Figs. 3(c)–3(l). These results indicate that a threshold for NV center creation by single-pulse irradiation exists between $F = 1.1$ and 1.8 J/cm^2. Our estimation is consistent with the typical graphitization threshold for a femtosecond laser pulse.[43–47] In addition, when the fluence was increased, the region's size also increased while the focal spot size [Fig. 3(m)] was maintained. Figure 3(n) shows the dependence of the fluence F on the diameter of the region. Here, the diameter was obtained by analyzing the edge position, which corresponds to the extremum of the first derivative for the radial direction of the PL intensity distribution. The diameter became larger than the fs-laser focal spot size (41 μm) at $F = 9.6$ J/cm^2 and reached 100 μm at $F = 54$ J/cm^2. In Fig. 3(n), we also show the increased NV concentration in each region. This concentration was obtained as follows: first, the background signal was subtracted from the photon count for each pixel in the region, where the background was defined as the average over 10×10 pixels on the right-top of each confocal image. Then, the photon count was averaged over the region of increased intensity. Finally, the count was divided by the effective focal volume. The NV concentration started to increase at $F = 1.8$ J/cm^2 and gradually became relatively constant at $F \sim 10$ J/cm^2 while repeatedly rising and falling. A single pulse with sufficient fluence will generate NV centers on a diamond surface over a wide region.

A single laser pulse with high fluence beyond the diamond graphitization threshold generates an NV-center-fabricated region over the focal spot size. Although the details of the mechanism are still under discussion, some possible factors, such as laser-produced plasma and induced shockwave, may relate to the NV centers' creation. When a high-intense pulse is focused on a material surface, the surface is subject to photon-radiation pressure. The pressure P_P is estimated by $P_P \sim I_P/c = F/cw_P$, where I_P is the peak
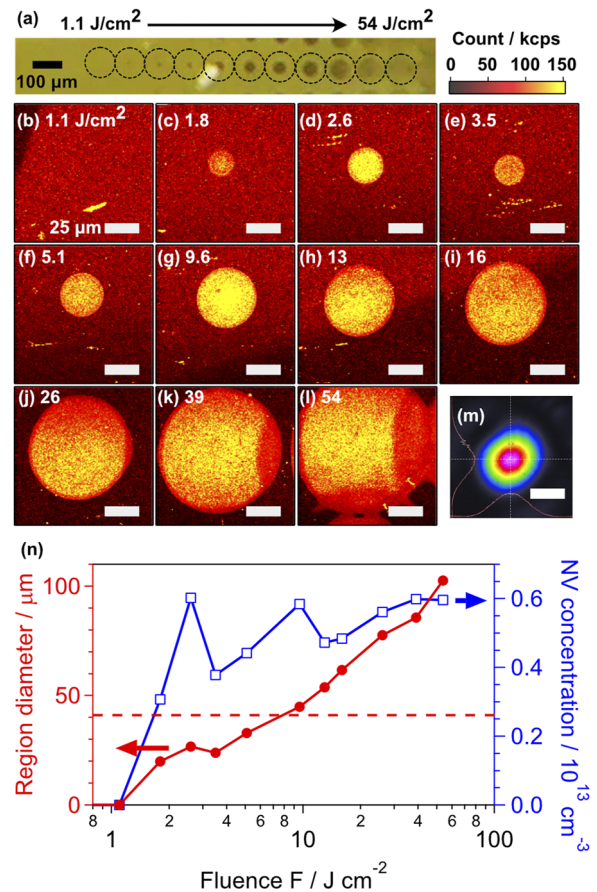

FIG. 3. (a) Series of fs-laser irradiated regions with various laser fluences F. (b)–(l) Confocal images at the circular-spot-irradiated regions in the range $F = 1.1$–54 J/cm^2. The pulse number N was fixed at 1 in each region. (m) Same as Fig. 1(b). (n) Dependence of F on the diameter (red filled circle) and on the increased NV concentration (blue unfilled square) in the region when the number of NV centers increased. The focal spot diameter, $2w = 41$ μm, is depicted as a red dotted line.

intensity, c is the speed of light, F is the fluence, and w_P is the pulse width. For the laser pulse with $F = 10$ J/cm^2 and $w_P = 35$ fs ($I_P = 3 \times 10^{14}$ W/cm^2), P_P impulsively reaches 10 GPa. Then, the laser pulse creates a high-dense plasma and laser ablation occurs.[49] During the process, the diamond also experiences high recoiled pressure by laser-ablated defects P_r. According to the study of femtosecond-laser-driven shockwave for Al film[50] and Si materials,[51] P_r is an order of 10–100 GPa for $I_P \sim 10^{14}$–10^{15} W/cm^2. The diamond will also be subject to high pressure. Depending on the laser fluence, the plasma distribution and shockwave propagation induced by such high pressure may assist the N-V formation at the laser-irradiated region. In the current study, plasma formation will occur not only at the diamond surface but also in the air region just above the surface. The maximum intensity reached 1.5×10^{15} W/cm^2 ($F = 54$ J/cm^2) at the focal position. According to the Coulomb-barrier suppression theory,[52] the ionization thresholds for ambient molecules (O$_2$ and N$_2$) can be calculated as 8.4×10^{13} and 2.4×10^{14} W/cm^2,

respectively.[52,53] Hence, the air molecules just above the diamond surface will also be ionized by the intense laser field and induce a plasma state.[54,55] The laser-induced plasma in the air also expands with supersonic velocity and drives shockwaves, which may relate to the NV creation.

C. Creation of NV centers in a millimeter-sized region

The results shown in Fig. 3 inspired us to create NV centers in a millimeter-sized region for single-shot irradiation. In Fig. 3(l), we showed the results for laser pulse irradiation with a spot diameter $2w$ (= $2w_x = 2w_y$) of 41 μm and a fluence F of 54 J/cm^2. The pulse energy E corresponds to 0.36 mJ, derived from a simple Gaussian distribution $F = E/(\pi w^2/2)$. After upgrading the CPA system, our current maximum pulse energy reached 500 mJ.[36] Applying the maximum energy gives a laser pulse with a larger focal spot and a higher fluence. Figure 4 shows the relation between $2w$ and F for a given E. For example, for F fixed at 54 J/cm^2, $2w$ increases from 41 to 1540 μm when E is increased from 0.36 to 500 mJ (from the blue-filled circle to the red-unfilled circle in Fig. 4). In addition, with sufficient laser fluence, the region containing NV centers is larger than the spot diameter, as shown in Fig. 3(n). Therefore, single-shot laser irradiation can create NV centers in a region with a diameter larger than 1.5 mm. Reducing the fluence while keeping the pulse energy fixed will increase the spot diameter. For the next example, we consider a laser pulse with F = 9.6 J/cm^2 and $2w$ = 41 μm (giving E = 0.064 mJ). Under these conditions, the NV-center-created region became almost as wide as the focal spot. If the fluence F is fixed at 9.6 J/cm^2, the beam diameter increases to $2w$ = 3640 μm at E = 500 mJ (from the blue-filled square to the red-unfilled square). When the fluence is larger than the estimated threshold for NV creation (in this case,
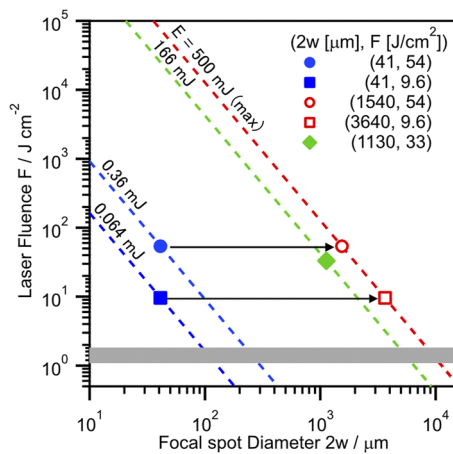
F = 1.1–1.8 J/cm^2, indicated by the gray bar), a single laser pulse with a sufficiently large spot diameter will generate NV centers over a millimeter-sized region.

Based on the above-mentioned discussion, we prepared a laser pulse of several hundred mJ. However, we must change experimental conditions to use such a high-energy pulse. When a high-energy pulse goes through the air atmosphere, it interacts with air molecules via non-linear optical processes, deteriorating the pulse quality. We must carry out such a high-energy experiment in a vacuum (~5 × 10^{-2} Pa) [Fig. 5(a)]. In addition, to obtain the high energy while suppressing the laser damage to the optics, the beam diameter was expanded to 50 mm. If the parabolic mirror with f = 165 mm focuses this laser beam, the NA becomes 0.15. The left side of Fig. 5(b) shows the beam profile at the focal position. The spot size diameter ($2w_x$, $2w_y$) became (5.7, 4.8 μm). Since the ideal spot size is calculated to be about 7 μm (in the case of the Airy disk diameter $2w$ of the diffraction-limited spot at a uniformly-illuminated beam, $2w$ = 1.22λ/NA), our laser beam was well-focused. Then we observed the beam profile at the defocused position. For example, the right side of Fig. 5(b) shows the profile at the position about 5 mm behind the focus. We confirmed the defocused spot diameter was about 1.5 mm, enough size to perform the irradiation experiments.

In the actual irradiation experiment, we applied pulse energy E = 166 mJ and defocused spot diameter $2w$ = 1.13 mm (the defocused position was set to 3.7 mm). Here, the diameter was confirmed by the irradiation mark on an aluminum plate before conducting the diamond irradiation experiments. The upper side of Fig. 5(c) shows the micrograph after the single pulse irradiation on diamond substrate No. 3. The irradiated region pattern reflects the laser intensity distribution, as shown on right side of Fig. 5(b). The region diameter of 1.08 mm, judging from the microscope scale bar, was consistent with the above-estimated diameter. Although the intensity distribution was neither uniform nor Gaussian, we estimated the fluence F of 33 J/cm^2 according to the same procedure discussed in Fig. 4 (the green-filled diamond). The estimated fluence was much higher than the graphitization threshold and enough for the high-fluence experiment. The lower side of Fig. 5(c) shows the micrograph after boiling acid treatment. Although some shaded pattern remained, almost all of the laser-induced defects were removed.

Figure 5(d) shows a series of confocal images at several regions on substrate No. 3. While the substrate is 2 mm square, the region that can sweep at one time is only 100 μm square. It is not practical to measure the entire substrate. Hence, we measured only 35 images to evaluate the size of the PL-increased region and the difference between the irradiated and non-irradiated regions. We first measured one of the four corners as a reference position. Then we measured several images for other regions by changing the lateral position using the two-axis micrometer attached to the sample stage. Here, the mirrored and tilted image of Fig. 5(c) is also overlapped in the background to clarify to compare the confocal image position with the laser-irradiated region. Judging from the boundary shape of the PL-increased region, the size of the PL-increased region was consistent with that of the laser-irradiated region. In addition, no particular PL increase was observed outside the laser-irradiated region. Figure 5(e) is an image of the area A shown in Fig. 5(d). We can confirm a part of the boundary area of the PL-increased region. Figure 5(f) shows the PL spectra measured at points A-1 to

FIG. 4. Estimated laser spot size at the maximum laser pulse energy. The dotted lines show the relationship between the focal spot diameter $2w$ and the laser fluence F at a given pulse energy E, given by $F = E/(\pi\omega^2/2)$. The blue-filled circle and square are examples of the relation ($2w$, F) at the same experimental conditions as in Figs. 3(g)–3(l), respectively. These values move to the positions of the red-unfilled circle and square if the maximum energy E = 500 mJ is applied while keeping the fluence constant. The green-filled diamond shows the relation ($2w$, F) if $2w$ is assumed to be 1.13 mm for E = 166 mJ. The gray bar shows the estimated threshold for NV center production by single-shot irradiation.
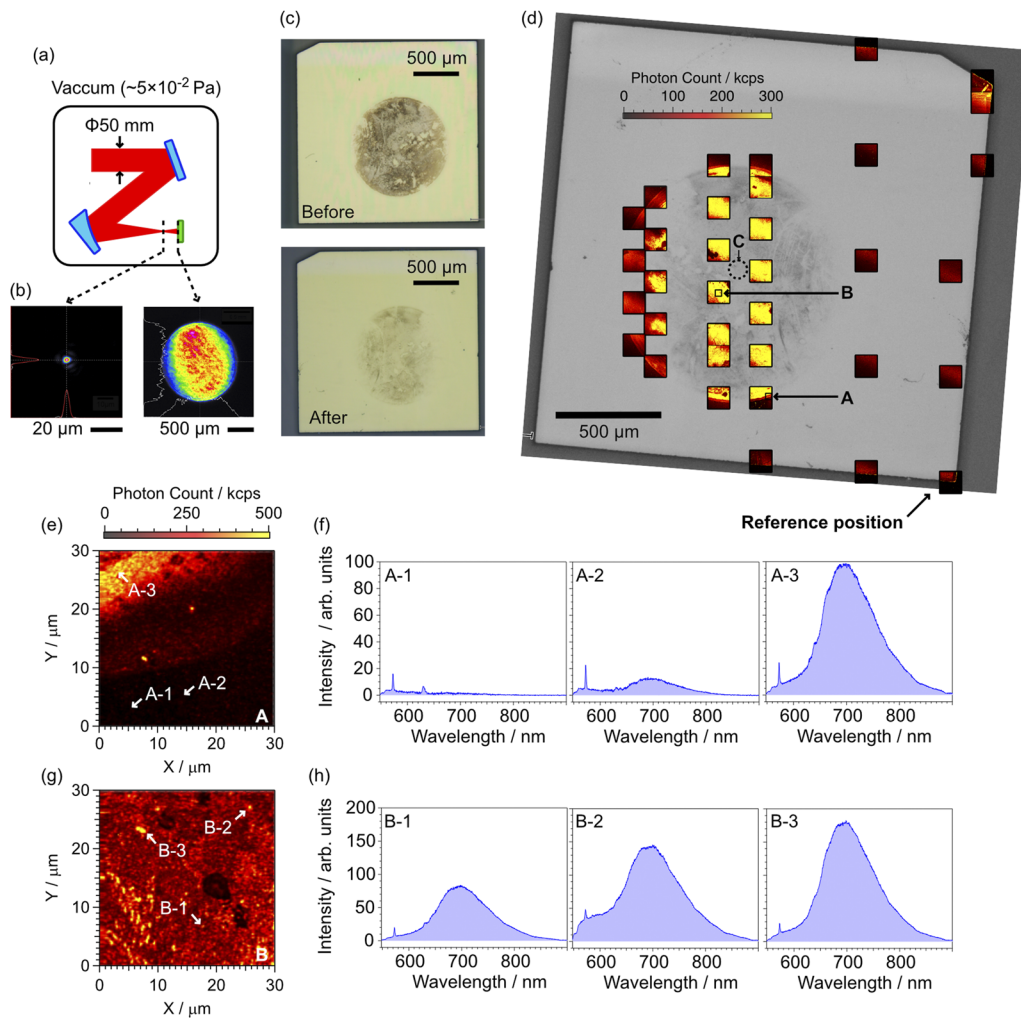
FIG. 5. (a) Setup for irradiation with a high-energy ultrashort laser pulse. (b) Typical beam profiles at the focal plane (left) and at a defocused plane (right). (c) Micrographs of the laser-irradiated diamond substrate before (upper) and after (lower) the hot-acid treatment. (d) Confocal images at several positions on the diamond substrate. The image of one of the four corners was used as a reference position. Then, several images were measured by adjusting the lateral position with the two-axis micrometer attached to the sample stage. Each confocal image is 100 μm square. The mirrored and tilted image of Micrograph (c) is displayed in the background. (e) and (g) Confocal images of areas A and B depicted in (d). (f) and (h) PL spectra measured at the points depicted in (e) and (g).

A-3, indicated in Fig. 5(e). Points A-1 and A-2 were selected in the unirradiated region. Point A-1 showed a typical spectrum on the pristine diamond surface and did not include the NV center's signal. In some cases, we found NV centers' signal like the A-2's PL spectrum. Point A-3 was inside the irradiated region. The A-3's spectrum shows a strong NV centers' signal, about one-order higher than the A-2's spectrum. Figure 5(g) is a close-up of area B in Fig. 5(d), showing the vicinity of the center in the irradiated region. Although the PL intensity did not uniformly distribute, the entire intensity became much higher than that of the unirradiated region. The distribution may reflect several factors, such as the laser profile, the local structure of the diamond surface, and local nitrogen distribution. We also confirmed PL spectra at several points (B-1 to B-3) as shown in Fig 5(f), and all the data showed strong signals from NV centers. For

example, the PL intensity at point B-3 is more than ten times larger than that of a single NV center, and the corresponding concentration is at least $>5 \times 10^{13}$ cm^{-3}. Combined with the results of spin coherence time measurements discussed in Sec. III D, we conclude that a single-shot femtosecond laser pulse created NV centers in a millimeter-sized region.

In this experiment, the estimated laser fluence was higher than 10 J/cm^2, which suggests the PL-increased region may expand compared with the laser-irradiated region, as shown in Fig. 3(l). Nevertheless, the size of the PL-increased region almost coincided with that of the laser-irradiated region. One of the differences in the experimental conditions between Figs. 3 and 5 is whether the sample-surrounding environment is in an air atmosphere or a vacuum. As mentioned in Sec. III B, the presence of a laser-induced

plasma shock wave caused by air breakdown may affect the creation of NV centers' around the laser-irradiated region. As another possible reason, an air atmosphere may affect the propagation direction of a shock wave induced on a diamond surface. In any case, the creation of NV centers was realized in a vacuum. We are continuing our investigations into controlling the NV center density and the region's size.

D. Electron-spin coherence time

The electron-spin coherence time T_2 and free induction decay (FID) time T_2^* are directly related to the required sensitivity for AC and DC quantum sensing applications.[4,6,26–28] We finally measured T_2 and T_2^* at the fs-laser-irradiated regions using a spin-echo sequence and a Ramsey sequence. To measure T_2 and T_2^*, we applied microwave irradiation to the NV centers using a Cu wire with a diameter of 30 μm placed over the diamond substrate [Fig. 6(a), left side]. A static magnetic field B_0 was applied along one of four possible N-V axes using a permanent magnet. The right side of Fig. 6(a) shows a close-up confocal image of area C, in the vicinity of the center of the laser-irradiated region and close to (<100 μm) the Cu wire [area C is also shown in Fig. 5(d)]. Figure 6(b) shows the optically-detected magnetic resonance (ODMR) spectrum measured at point C-1 in area C. Four peaks split by the Zeeman effect due to the static field are observed. The peak at 2566 (3190) MHz corresponds to the transition between the electron spin states $|m_s = 0\rangle$ and $|m_s = -1\rangle$ ($|m_s = +1\rangle$) for the NV centers along the static field.[27] The B_0 was about 11.1 mT, estimated by using the Zeeman shifts of the two peaks (624 MHz = $2\gamma B_0$, where γ = 28.0 MHz/mT is the

electron gyromagnetic ratio). Using the NV centers with $|m_s = 0\rangle$ ↔ $|m_s = -1\rangle$ transition (indicated by black arrow), Rabi oscillation of the electron spins was observed to determine the lengths of the π and $\pi/2$ pulses [Fig. 6(c)]. Then, we measured spin-echo signals and obtained T_2 [Fig. 6(d)]. To remove common-mode noise, the measured S_0 (rotational axis of the second $\pi/2$ pulse parallel to that of the first $\pi/2$ pulse) and S_1 (antiparallel) were subtracted and normalized as $(S_0 - S_1)/(S_0 + S_1)$.[6,56] Then, T_2 was obtained by fitting to an exponential decay function ($\propto \exp\left[-(2\tau/T_2)\right]^n$), where 2τ is the time between the first and second $\pi/2$ pulses. We measured T_2 at three different points in this region, and the average value was 1.2 μs. We also measured T_2 at three points in the laser-irradiated region with F = 9.6 J/cm^2 [Fig. 3(g)] and the pristine (non-laser-irradiated) region, and the average T_2 became 1.0 and 1.2 μs, respectively. According to previous studies, T_2 for an ensemble of NV centers scales with the nitrogen concentration [N].[28] Based on the nitrogen content of our sample ([N] ~ 100 ppm), the expected T_2 was 1–2 μs. Our results are consistent with the results of previous research, indicating that P1 centers (substitutional nitrogen atoms) deteriorate the spin coherence of the NV centers. We also measured T_2^* by Ramsey sequence at the laser-irradiated region [Fig. 6(e)].[28] The T_2^* was determined by fitting the FID signal to an exponential decay function ($\propto \exp\left[-(\tau/T_2^*)\right]^n$), where τ is the time between the first and second $\pi/2$ pulses. The average value at three different points was 45 ns, which is also consistent with the expected T_2^* (~100 ns at [N] ~ 100 ppm).[28] These results indicate that the laser ablation and subsequent surface treatment will not influence the lengths of T_2 and T_2^*. This is beneficial for quantum applications with high sensitivity.
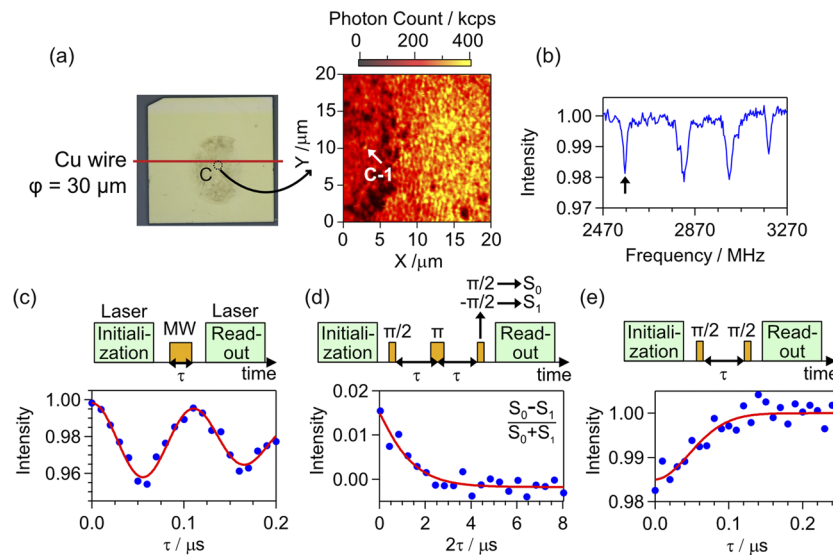

FIG. 6. (a) (Left) Diamond substrate with a Cu wire to apply microwave irradiation. (Right) Close-up confocal image at area C, in the vicinity of the center of the laser irradiated region and close to the Cu wire [same as area C depicted in Fig. 5(d)]. (b) CW-ODMR spectrum at point C-1 in area C, depicted in Fig. (a). A static magnetic field of 11.1 mT was applied along one of the possible NV axes. (c) Rabi oscillation pulse sequence (upper) and signal at point C-1 (lower). Based on a sinusoidal curve fit, the lengths of the $\pi/2$ and π pulses were determined. The π pulse length was 60 ns. (d) Spin-echo pulse sequence (upper) and the signal measured at point C-1 (lower). The details of the data analysis are explained in the main text. The T_2 became 1.3 ± 0.2 μs. (e) Ramsey-sequence (upper) and the FID signal (lower). This data was measured at another point close to C-1. The T_2^* became 68 ± 9 ns. Data in (c)–(e) are shown as blue dots and the curve fits as red curves.

IV. CONCLUSION

In summary, the generation of NV centers in synthetic bulk diamond was investigated using high-fluence and large-spot femtosecond laser pulses. NV centers were effectively created by single-pulse irradiation. Two focused-spot shapes, circular and linear, were investigated; the latter may be useful to create NV centers rapidly over a large region without post-annealing by line scanning. The size of the created region was expanded for a higher laser fluence, probably due to laser–diamond surface and laser–air interactions. Furthermore, the NV center creation over a millimeter-sized spot was demonstrated by a large defocused spot in a vacuum condition. We expect that a raster scanning of the defocused spot with a suitable mask generates NV centers over a centimeter-sized region in a short time. The spin-echo and FID signals showed that P1 centers restricted the length of T_2 and $T_2{}^*$ for the irradiated region, and single-pulse laser ablation had little influence on T_2 and $T_2{}^*$.

The three-dimensional (3D) formation of high-dense NV centers will be the next step to realize the high-sensitive quantum sensor by laser irradiation. So far, NV center formation over a large region has been limited to a few methods, such as electron irradiation and chemical vapor deposition. The present study showed that the laser scanning of a linear spot might realize the rapid creation of NV centers in a 3D region. The ultrashort laser irradiation method may pave the way for a new approach to creating NV centers over a wide region.

ACKNOWLEDGMENTS

AUTHOR DECLARATIONS

Conflict of Interest

The authors have no conflicts to disclose.

Author Contributions

Masanori Fujiwara: Formal analysis (equal); Investigation (equal); Writing – original draft (equal). **Shunsuke Inoue**: Data curation (equal); Formal analysis (equal); Investigation (equal). **Shin-ichiro Masuno**: Formal analysis (supporting); Investigation (supporting). **Haining Fu**: Investigation (supporting). **Shigeki Tokita**: Project administration (supporting); Resources (equal). **Masaki Hashida**: Formal analysis (equal); Investigation (supporting); Methodology (equal); Validation (equal); Writing – original draft (supporting). **Norikazu Mizuochi1**: Funding acquisition (equal); Project administration (equal); Supervision (lead); Writing – review & editing (lead).

DATA AVAILABILITY

The data that support the findings of this study are available from the corresponding author upon reasonable request.

REFERENCES

[1]T. D. Ladd, F. Jelezko, R. Laflamme, Y. Nakamura, C. Monroe, and J. L. O'Brien, "Quantum computers," Nature **464**, 45 (2010).

[2]I. Aharonovich, D. Englund, and M. Toth, "Solid-state single-photon emitters," Nat. Photonics **10**, 631 (2016).

[3]S. Pezzagna and J. Meijer, "Quantum computer based on color centers in diamond," Appl. Phys. Rev. **8**, 011308 (2021).

[4]L. Rondin, J.-P. Tetienne, T. Hingant, J.-F. Roch, P. Maletinsky, and V. Jacques, "Magnetometry with nitrogen-vacancy defects in diamond," Rep. Prog. Phys. **77**, 056503 (2014).

[5]M. W. Doherty, N. B. Manson, P. Delaney, F. Jelezko, J. Wrachtrup, and L. C. L. Hollenberg, "The nitrogen-vacancy colour centre in diamond," Phys. Rep. **528**, 1 (2013).

[6]E. D. Herbschleb, H. Kato, Y. Maruyama, T. Danjo, T. Makino, S. Yamasaki, I. Ohki, K. Hayashi, H. Morishita, M. Fujiwara, and N. Mizuochi, "Ultra-long coherence times amongst room temperature solid-state spins," Nat. Commun. **10**, 3766 (2019).

[7]J. M. Taylor, P. Cappellaro, L. Childress, L. Jiang, D. Budker, P. R. Hemmer, A. Yacoby, R. Walsworth, and M. D. Lukin, "High-sensitivity diamond magnetometer with nanoscale resolution," Nat. Phys. **4**, 810 (2008).

[8]G. Balasubramanian, I. Y. Chan, R. Kolesov, M. Al-Hmoud, J. Tisler, C. Shin, C. Kim, A. Wojcik, P. R. Hemmer, A. Krueger, T. Hanke, A. Leitenstorfer, R. Bratschitsch, F. Jelezko, and J. Wrachtrup, "Nanoscale imaging magnetometry with diamond, spins under ambient conditions," Nature **455**, 648 (2008).

[9]J. R. Maze, P. L. Stanwix, J. S. Hodges, S. Hong, J. M. Taylor, P. Cappellaro, L. Jiang, M. V. G. Dutt, E. Togan, A. S. Zibrov, A. Yacoby, R. L. Walsworth, and M. D. Lukin, "Nanoscale magnetic sensing with an individual, electronic spin in diamond," Nature **455**, 644 (2008).

[10]F. Dolde, H. Fedder, M. W. Doherty, T. Nöbauer, F. Rempp, G. Balasubramanian, T. Wolf, F. Reinhard, L. C. L. Hollenberg, F. Jelezko, and J. Wrachtrup, "Electric-field sensing using single diamond spins," Nat. Phys. **7**, 459 (2011).

[11]G. Kucsko, P. C. Maurer, N. Y. Yao, M. Kubo, H. J. Noh, P. K. Lo, H. Park, and M. D. Lukin, "Nanometre-scale thermometry in a living cell," Nature **500**, 54 (2013).

[12]K. Hayashi, Y. Matsuzaki, T. Taniguchi, T. Shimo-Oka, I. Nakamura, S. Onoda, T. Ohshima, H. Morishita, M. Fujiwara, S. Saito, and N. Mizuochi, "Optimization of temperature sensitivity using the optically detected magnetic-resonance spectrum of a nitrogen-vacancy center ensemble," Phys. Rev. Appl. **10**, 034009 (2018).

[13]M. W. Doherty, V. V. Struzhkin, D. A. Simpson, L. P. McGuinness, Y. Meng, A. Stacey, T. J. Karle, R. J. Hemley, N. B. Manson, L. C. L. Hollenberg, and S. Prawer, "Electronic properties and metrology applications of the diamond NV–center under pressure," Phys. Rev. Lett. **112**, 047601 (2014).

[14]T. Fujisaku, R. Tanabe, S. Onoda, R. Kubota, T. F. Segawa, F. T.-K. So, T. Ohshima, I. Hamachi, M. Shirakawa, and R. Igarashi, "pH nanosensor using electronic spins in diamond," ACS Nano **13**, 11726 (2019).

[15]E. D. Herbschleb, H. Kato, T. Makino, S. Yamasaki, and N. Mizuochi, "Ultra-high dynamic range quantum measurement retaining its sensitivity," Nat. Commun. **12**, 306 (2021).

[16]Y.-C. Chen, P. S. Salter, S. Knauer, L. Weng, A. C. Frangeskou, C. J. Stephen, S. N. Ishmael, P. R. Dolan, S. Johnson, B. L. Green, G. W. Morley, M. E. Newton, J. G. Rarity, M. J. Booth, and J. M. Smith, "Laser writing of coherent colour centres in diamond," Nat. Photonics **11**, 77 (2017).

[17]Y.-C. Chen, B. Griffiths, L. Weng, S. S. Nicley, S. N. Ishmael, Y. Lekhai, S. Johnson, C. J. Stephen, B. L. Green, G. W. Morley, M. E. Newton, M. J. Booth, P. S. Salter, and J. M. Smith, "Laser writing of individual nitrogen-vacancy defects in diamond with near-unity yield," Optica **6**, 662 (2019).

[18]C. J. Stephen, B. L. Green, Y. N. D. Lekhai, L. Weng, P. Hill, S. Johnson, A. C. Frangeskou, P. L. Diggle, Y. C. Chen, M. J. Strain, E. Gu, M. E. Newton, J. M. Smith, P. S. Salter, and G. W. Morley, "Deep three-dimensional solid-state qubit arrays with long-lived spin coherence," Phys. Rev. Appl. **12**, 064005 (2019).

[19]B. Griffiths, A. Kirkpatrick, S. S. Nicley, R. L. Patel, J. M. Zajac, G. W. Morley, M. J. Booth, P. S. Salter, and J. M. Smith, "Microscopic processes during ultrafast laser generation of Frenkel defects in diamond," Phys. Rev. B **104**, 174303 (2021).

[20] J. M. Smith, S. A. Meynell, A. C. Bleszynski Jayich, and J. Meijer, "Colour centre generation in diamond for quantum technologies," Nanophotonics **8**, 1889 (2019).

[21] V. Yurgens, J. A. Zuber, S. Flågan, M. de Luca, B. J. Shields, I. Zardo, P. Maletinsky, R. J. Warburton, and T. Jakubczyk, "Low-Charge-noise nitrogen-vacancy centers in diamond created using laser writing with a solid-immersion lens," ACS Photonics **8**, 1726 (2021).

[22] X. J. Wang, H. H. Fang, F. W. Sun, and H. B. Sun, "Laser writing of color centers," Laser Photonics Rev. **16**, 2100029 (2021).

[23] X. Gao, S. Pandey, M. Kianinia, J. Ahn, P. Ju, I. Aharonovich, N. Shivaram, and T. Li, "Femtosecond laser writing of spin defects in hexagonal boron nitride," ACS Photonics **8**, 994 (2021).

[24] S. Castelletto, J. Maksimovic, T. Katkus, T. Ohshima, B. C. Johnson, and S. Juodkazis, "Color centers enabled by direct femto-second laser writing in wide bandgap semiconductors," Nanomaterials **11**, 72 (2021).

[25] Y.-C. Chen, P. S. Salter, M. Niethammer, M. Widmann, F. Kaiser, R. Nagy, N. Morioka, C. Babin, J. Erlekampf, P. Berwian, M. J. Booth, and J. Wrachtrup, "Laser writing of scalable single color centers in silicon carbide," Nano Lett. **19**, 2377 (2019).

[26] S. Choi, J. Choi, R. Landig, G. Kucsko, H. Zhou, J. Isoya, F. Jelezko, S. Onoda, H. Sumiya, V. Khemani, C. von Keyserlingk, N. Y. Yao, E. Demler, and M. D. Lukin, "Observation of discrete time-crystalline order in a disordered dipolar many-body system," Nature **543**, 221 (2017).

[27] E. V. Levine, M. J. Turner, P. Kehayias, C. A. Hart, N. Langellier, R. Trubko, D. R. Glenn, R. R. Fu, and R. L. Walsworth, "Principles and techniques of the quantum diamond microscope," Nanophotonics **8**, 1945 (2019).

[28] E. Bauch, S. Singh, J. Lee, C. A. Hart, J. M. Schloss, M. J. Turner, J. F. Barry, L. M. Pham, N. Bar-Gill, S. F. Yelin, and R. L. Walsworth, "Decoherence of ensembles of nitrogen-vacancy centers in diamond," Phys. Rev. B **102**, 134210 (2020).

[29] T. Wolf, P. Neumann, K. Nakamura, H. Sumiya, T. Ohshima, J. Isoya, and J. Wrachtrup, "diamond magnetometry," Phys. Rev. X **5**, 041001 (2015).

[30] J. F. Barry, M. J. Turner, J. M. Schloss, D. R. Glenn, Y. Song, M. D. Lukin, H. Park, and R. L. Walsworth, "Optical magnetic detection of single-neuron action potentials using quantum defects in diamond," Proc. Natl. Acad. Sci. U. S. A. **113**, 14133 (2016).

[31] C. L. Degen, F. Reinhard, and P. Cappellaro, "Quantum sensing," Rev. Mod. Phys. **89**, 035002 (2017).

[32] S. C. Scholten, A. J. Healey, I. O. Robertson, G. J. Abrahams, D. A. Broadway, and J.-P. Tetienne, "Widefield quantum microscopy with nitrogen-vacancy centers in diamond: Strengths, limitations, and prospects," J. Appl. Phys. **130**, 150902 (2021).

[33] K. Arai, A. Kuwahata, D. Nishitani, I. Fujisaki, R. Matsuki, Y. Nishio, Z. Xin, X. Cao, Y. Hatano, S. Onoda, C. Shinei, M. Miyakawa, T. Taniguchi, M. Yamazaki, T. Teraji, T. Ohshima, M. Hatano, M. Sekino, and T. Iwasaki, "Millimetre-scale magnetocardiography of living rats with thoracotomy," Commun. Phys. **5**, 200 (2022).

[34] T. Kurita, Y. Shimotsuma, M. Fujiwara, M. Fujie, N. Mizuochi, M. Shimizu, and K. Miura, "Direct writing of high-density nitrogen-vacancy centers inside diamond by femtosecond laser irradiation," Appl. Phys. Lett. **118**, 214001 (2021).

[35] V. V. Kononenko, I. I. Vlasov, V. M. Gololobov, T. V. Kononenko, T. A. Semenov, A. A. Khomich, V. A. Shershulin, V. S. Krivobok, and V. I. Konov, "Nitrogen-vacancy defects in diamond produced by femtosecond laser nanoablation technique," Appl. Phys. Lett. **111**, 081101 (2017).

[36] S. Inoue, S. Sakabe, Y. Nakamiya, and M. Hashida, "Jitter-free 40-fs 375-keV electron pulses directly accelerated by an intense laser beam and their application to direct observation of laser pulse propagation in a vacuum," Sci. Rep. **10**, 20387 (2020).

[37] C. Schreyvogel, V. Polyakov, R. Wunderlich, J. Meijer, and C. E. Nebel "Active charge state control of single NV centres in diamond by in-plane Al-Schottky junction," Sci. Rep. **5** 12160 (2015).

[38] G. Davies, "Vibronic spectra in diamond," J. Phys. C: Solid State Phys. **7**, 3797 (1974).

[39] A. Gruber, A. Dräbenstedt, C. Tietz, L. Fleury, J. Wrachtrup, and C. von Borczyskowski, "Scanning confocal optical microscopy and magnetic resonance of single defect centers," Science **276**, 2012 (1997).

[40] S. Karaveli, O. Gaathon, A. Wolcott, R. Sakakibara, O. A. Shemesh, D. S. Peterka, E. S. Boyden, J. S. Owen, R. Yuste, and D. Englund, "Modulation of nitrogen vacancy charge state and fluorescence in nanodiamonds using electrochemical potential," Proc. Natl. Acad. Sci. U. S. A. **113**, 3938 (2016).

[41] J. Jaske, D. W. M. Lau, X. Vidal, L. P. McGuinness, P. Reineck, B. C. Johnson, M. W. Doherty, J. C. McCallum, S. Onoda, F. Jelezko, T. Ohsima, T. Volz, J. H. Cole, B. C. Gibson, and A. D. Greentree, "Stimulated emission from nitrogen-vacancy centres in diamond," Nat. Commun. **8**, 14000 (2017).

[42] E. Fraczek, V. G. Savitski, M. Dale, B. G. Breeze, P. Diggle, M. Markham, A. Bennett, H. Dhillon, M. E. Newton, and A. J. Kemp, "Laser spectroscopy of NV−and NV0 colour centres in synthetic diamond," Opt. Mater. Express **7**, 2571 (2017).

[43] Y. Liu, G. Chen, M. Song, X. Ci, B. Wu, E. Wu, and H. Zeng, "Fabrication of nitrogen vacancy color centers by femtosecond pulse laser illumination," Opt. Express **21**, 12843 (2013).

[44] V. V. Kononenko, V. M. Gololobov, and V. I. Konov, "Latent laser-induced graphitization of diamond," Appl. Phys. A **122**, 258 (2016).

[45] T. Kurita, N. Mineyuki, Y. Shimotsuma, M. Fujiwara, N. Mizuochi, M. Shimizu, and K. Miura, "Efficient generation of nitrogen-vacancy center inside diamond with shortening of laser pulse duration," Appl. Phys. Lett. **113**, 211102 (2018).

[46] P. Boerner, M. Hajri, N. Ackerl, and K. Wegener, "Experimental and theoretical investigation of ultrashort pulsed laser ablation of diamond," J. Laser Appl. **31**, 022202 (2019).

[47] B. Ali, H. Xu, D. Chetty, R. T. Sang, I. V. Litvinyuk, and M. Rybachuk, "Laser-induced graphitization of diamond under 30 fs laser pulse irradiation," J. Phys. Chem. Lett. **13**, 2679 (2022).

[48] S. I. Kudryashov, A. A. Ionin, S. V. Makarov, N. N. Mel'Nik, L. V. Seleznev, and D. V. Sinitsyn, "Femtosecond laser ablation of carbon: From spallation to formation of hot critical plasma," AIP Conf. Proc. **1464**, 244 (2012).

[49] B. Ali, I. V. Litvinyuk, and M. Rybachuk, "Femtosecond laser micromachining of diamond: Current research status, applications and challenge," Carbon **179**, 209 (2021).

[50] R. Evans, A. D. Badger, F. Falliès, M. Mahdieh, T. A. Hall, P. Audebert, J.-P. Geindre, J.-C. Gauthier, A. Mysyrowicz, G. Grillon, and A. Antonetti, "Time- and space-resolved optical probing of femtosecond-laser-driven shock waves in aluminum," Phys. Rev. Lett. **77**, 3359 (1996).

[51] M. Tsujino, T. Sano, O. Sakata, N. Ozaki, S. Kimura, S. Takeda, M. Okoshi, N. Inoue, R. Kodama, K. F. Kobayashi, and A. Hirose, "Synthesis of submicron metastable phase of silicon using femtosecond laser-driven shock wave," J. Appl. Phys. **110**, 126103 (2011).

[52] S. Augst, D. D. Meyerhofer, D. Strickland, and S. L. Chin, "Laser ionization of noble gases by Coulomb-barrier suppression," J. Opt. Soc. Am. B **8**, 858 (1991).

[53] X. M. Tong, Z. X. Zhao, and C. D. Lin, "Theory of molecular tunneling ionization," Phys. Rev. A **66**, 033402 (2002).

[54] P. Sprangle, J. R. Peñano, and B. Hafizi, "Propagation of intense short laser pulses in the atmosphere," Phys. Rev. E **66**, 046418 (2002).

[55] B. Rethfeld, K. Sokolowski-Tinten, D. von der Linde, and S. I. Anisimov, "Timescales in the response of materials to femtosecond laser excitation," Appl. Phys. A **79**, 767 (2004).

[56] N. Bar-Gill, L. M. Pham, A. Jarmola, D. Budker, and R. L. Walsworth, "Solid-state electronic spin coherence time approaching one second," Nat.Commun. **4**, 1743 (2013).